Applied Radiation and Isotopes 67 (2009) 1912–1918

Contents lists available at ScienceDirect

Applied Radiation and Isotopes

journal homepage: www.elsevier.com/locate/apradiso

Unfolding the neutron spectrum of a NE213 scintillator using artificial neural networks

A. Sharghi Ido [a], M.R. Bonyadi [b], G.R. Etaati [c], M. Shahriari [a,*]

[a] Radiation Application Department, Shahid Beheshti University, Tehran, Iran
[b] Electrical and Computer Engineering Faculty, Shahid Beheshti University, Tehran, Iran
[c] Nuclear Engineering and Physics Faculty, Amir Kabir University of Technology, Tehran, Iran

ARTICLE INFO

Article history:
Received 19 July 2008
Received in revised form
19 May 2009
Accepted 27 May 2009

PACS:
07.05.Mh
29.40.Mc
02.30.Zz
05.10.Ln

Keywords:
Neutron spectrum unfolding
SCINFUL
FORIST
Artificial neural network
Scintillation detector

ABSTRACT

Artificial neural networks technology has been applied to unfold the neutron spectra from the pulse height distribution measured with NE213 liquid scintillator. Here, both the single and multi-layer perceptron neural network models have been implemented to unfold the neutron spectrum from an Am–Be neutron source. The activation function and the connectivity of the neurons have been investigated and the results have been analyzed in terms of the network's performance. The simulation results show that the neural network that utilizes the Satlins transfer function has the best performance. In addition, omitting the bias connection of the neurons improve the performance of the network. Also, the SCINFUL code is used for generating the response functions in the training phase of the process. Finally, the results of the neural network simulation have been compared with those of the FORIST unfolding code for both ^{241}Am–Be and ^{252}Cf neutron sources. The results of neural network are in good agreement with FORIST code.

1. Introduction

The unfolding of energy distribution of the neutron fluence, also known as the neutron spectrum, Φ_E (E), is imperative to various important radiation protection-related problems. For example, the neutron radiation dosimetry and shielding evaluation of nuclear facilities and the isotopic neutron sources, like ^{252}Cf, ^{241}AmBe, and, ^{239}PuBe, require knowledge of the neutron spectrum. Moreover, the accurate unfolding of the neutron spectra increases the sensitivity of the assays performed on the nuclear materials identification (Mullens et al., 2004).

In fast neutron spectroscopy, organic liquid scintillators are widely utilized due to the efficient neutron/gamma pulse-shape discrimination. In general, unfolding with this type of detector can be seen as a mapping from the n-dimensional space of the detector response the m-dimensional space of the neutron energy fluence (Burrus, 1976). To unfold the neutron spectra, several mathematical methods have been proposed, such as least-squares (Stallmann, 1985), iterative (Sanna, 1981) and Monte Carlo methods (Sanna and O'Brien, 1971).

Recently, artificial neural networks (ANNs) have been used to unfold the neutron spectra from Bonner sphere spectrometer count rates (Vega-Carrillo et al., 2006) and to perform neutron dosimetry (Avdic et al., 2006; Vega-Carrillo et al., 2007). In these cases, the spectrometer's detector was a ^{6}LiI (Eu) scintillator. The ANNs have also been utilized to unfold the neutron spectrum using the information provided by a small NE213 scintillator (Koohi-Fayegh et al., 1993).

1.1. Detector response matrix

The detector response, $R(H, E)$, the count rates, dN/dH, and the neutron spectrum, Φ_E (E), are related through the Fredholm integral equation of the first kind, as shown in Eq. (1)

$$\frac{dN}{dH} = \int_{E\min}^{E\max} R(H,E)\Phi_E(E)dE \quad (1)$$

Here, the dN/dH is recorded from any radiation detector and is the result of folding the detector's inherent response function and the energy distribution of the incident radiation. Because $R(H, E)$ and

* Corresponding author. Fax: +98 21 22431780.
E-mail address: m-shahriari@sbu.ac.ir (M. Shahriari).

0969-8043/$ - see front matter Crown Copyright © 2009 Published by Elsevier Ltd. All rights reserved.
doi:10.1016/j.apradiso.2009.05.020

dN/dH, that is obtained with a multichannel analyzer, have a discrete distribution Eq. (1) is solved in discrete form as shown:

$$N_i = \sum_j R_{i,j}\Phi_j \quad (2)$$

where N_i is the recorded count in the ith channel, $R_{i,j}$ is the response matrix, coupling the ith pulse height interval with the jth energy interval, and Φ_j is the radiation fluence in the jth energy interval (Johnson, 1975; Johnson et al., 1977; Knoll, 2000)

1.2. SCINFUL

The FORTRAN 77 code SCINFUL (scintillator full response to neutron detection) is a Monte Carlo simulation program written to compute the complete response of a scintillation detector (NE213 or NE110) to the incident neutrons of energy ranging from 0.1 up to 80 MeV (Dickens, 1988). The code can calculate the reaction position, and the energy and direction of scattered neutrons and secondary particles in the detector. SCINFUL includes 39 final reaction channels, starting from 11 initial reactions, i.e., H(n,p), C(n,n), C(n,n′), C(n,2n), C(n,p), C(n,np), C(n,d), C(n,^{3}He), C(n,α), C(n,n′3 α), C(n,t). When the reaction of a specific channel is not included in SCINFUL the contribution of this channel is calculated separately (Rasolonjatovo et al., 2002; Satoh et al., 2005) and is utilized in SCINFUL.

The large number of reaction channels is an advantage of SCINFUL, compared to other existing codes such as CECIL (Cecil et al., 1979). But, on the other hand, CECIL has the capability of producing the response functions for neutrons of energies up to about a few GeV. Recently, some improvements have been made to SCINFUL to calculate the detection efficiency for neutron energies up to 3 GeV (Satoh et al., 2005).

Some studies show the agreement between the results calculated by SCINFUL and other codes such as NRESP (Klein and Neumann, 2002). Also the comparison between the simulated response of a scintillation detector and the experimental data proves that the SCINFUL results show a better agreement compared with the CECIL results (Meigo, 1997).

The capabilities of SCINFUL for generating the neutron response functions are:

1) Source geometry: Only isotropic point source can be simulated.
2) Energy spectrum: The incident neutrons can be monoenergetic of chosen from uniform or Maxwellian energy distributions.

Fig. 1 shows a response matrix for the NE213 scintillator (5.1 ∅ × 5.1 cm^2) with 1 MeV energy resolution in the energy interval between 1 and 14 MeV, which was obtained with the SCINFUL code. The term MeV electron equivalent (MeVee) is a unit used to measure pulse height in the detector and it is the energy of an electron that gives the same light output (Knoll, 2000).

1.3. Artificial neural networks

Neural networks are composed of simple elements operating in parallel. These elements are inspired by the biological nervous system. As in nature, the network function is determined largely by the connections between elements.

One of the simplest neural networks, called perceptron (Rosenblatt, 1961), is a single-layer network, whose weights and biases can be trained to produce a correct target vector. The perceptron has generated a great interest due to its ability to generalize from its training vectors and learn from initially randomly distributed connections (Rosenblatt, 1961).

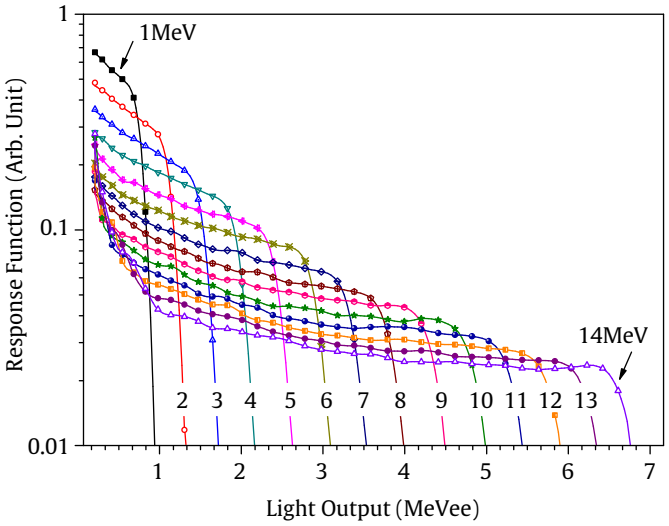

Fig. 1. A response matrix for the scintillator, generated by SCINFUL for energy range of 1–14 MeV.

Perceptrons are especially suited for the simple problems in pattern classification.

The neural networks require a training in which the learning of a network is the adaptation process to the data training, while the training is itself the adaptation process that makes learning possible. The training has the objective of selecting the weight that adapts better to the net in relation to the presented data, so that it carries out the desired function.

The aim of this work was to apply the ANNs to unfold the neutron spectrum using the pulse height spectrum from a NE213 and to study the effect of the transfer function in the ANN's performance. The final ANN algorithm was utilized to unfold the neutron spectra from ^{252}Cf and ^{241}Am–Be sources that were compared with the spectra unfolded with the FORIST (FERDOR with optimized resolution using iterative smoothing technique) unfolding code.

2. Methods

Here, the ANN performs a mapping of the measured detector data, N, to the neutron energy spectrum Φ , i.e. $\Phi = f(N)$, where f is a nonlinear energy transfer function. The ANN's output is shown (Rosenblatt, 1961):

$$\Phi_j = b_j + a_j\sigma\left\{\sum_{i=1}^{q} W_{i,j}\left[\sigma\sum_{i=1}^{q}\Omega_{i,k}N_k + B_i\right] + \beta_j\right\} \quad (3)$$

where the matrix $\Omega_{i,k}$ and the vector B_i represent the weights and biases of the hidden layer with q nodes, respectively, $W_{i,j}$ and β_j represent the weights and biases of the output layer, and a_j and b_j are scaling parameters. σ is the transfer function of the network. The index $j = 1, 2,\ldots,m$ is the number of neutron energy groups and the index $k = 1, 2\ldots,n$ is the number of pulse height distribution bins.

An important feature of the ANN performance is the transfer function utilized to activate the neurons. Available transfer functions are shown in Fig. 2 (Rosenblatt, 1961). After several trials it was found that using Satlins transfer function, defined in Eq. (4), results in the best performance of the ANN that was observed in a better convergence of the ANN, as can be noticed in Fig. 3. Fig. 3 denotes that the performances of the network, where its transfer function is Satlin, Purelin and Tansig

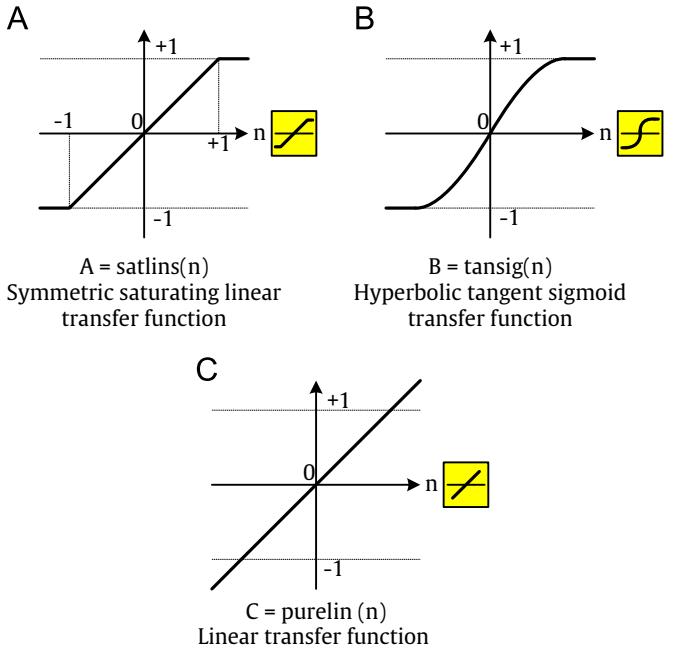

Fig. 2. Satlins (A), Tansig (B) and Pureline (C) transfer functions.

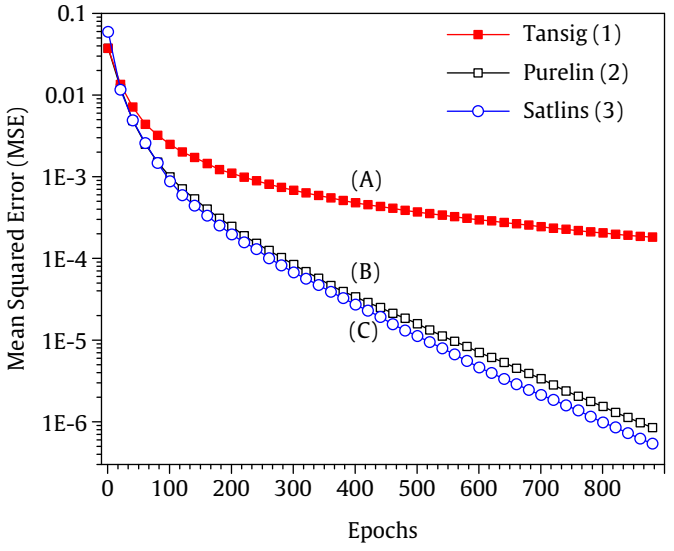

Fig. 3. Convergence of Tansig (A), Pureline (B) and Satlins (C) transfer functions.

are 8.41671×10^{-7}, 5.3825×10^{-7} and 1.81101×10^{-4}, respectively

$$f(x)\begin{cases} 1, & x > +1 \\ x, & -1 < x < +1 \\ -1, & x < -1 \end{cases} \quad (4)$$

According to Fig. 3 Satlin and Purelin are near together, but Satlin has better performance and has been chosen as transfer function. After choosing the transfer function, the network weights have to be modified. There are three categories of algorithms for the weight modification:

- Back propagation algorithm, which has the simplest implementation, by minimizing the performance function.
- Heuristic technique, developed from an analysis of the performance of the standard steepest descent algorithm.
- Standard numerical optimization techniques like conjugate gradient, quasi-Newton, and Levenberg–Marquardt (Hagan et al., 1996).

In this work, the Resilient back-propagation algorithm from the second category has been employed and the Matlab® Neural Network Toolbox (Demuth and Beale, 2002) was used to implement the neural networks.

2.1. Special features of the network

For a given $\Phi_E(E)$, the elements of the matrix R are varied to obtain a prediction of N with an acceptable error.

On the other hand, in linear neural nets, it is known that (Rosenblatt, 1961)

$$O_j = f\left(b_j \times \sum_i w_{ij} x_i\right) \quad (5)$$

where f is the transfer function of the neurons, O_j is the output of the jth output neuron, $w_{i,j}$ is the weight, which connects the ith input neuron to jth output neuron, b_i is a bias, and x_i is the input of the ith neuron in input layer.

The functions f may be chosen by different methods. The Tansig (sigmoid tangent), Purelin and Satlins (Eq. (5)) are mostly used for the activation part of the neurons (see Fig. 2).

Considering Eqs. (2) and (5), the network needs a linear transfer function for a direct mapping of any variation in the input of the network to its output. The root mean square error (*MSE*) was utilized to compare the original spectrum ($\Phi_E(E)^{ORIGINAL}$) with the ANN ($\Phi_E(E)^{ANN}$) unfolded spectrum, as shown (Vega-Carrillo

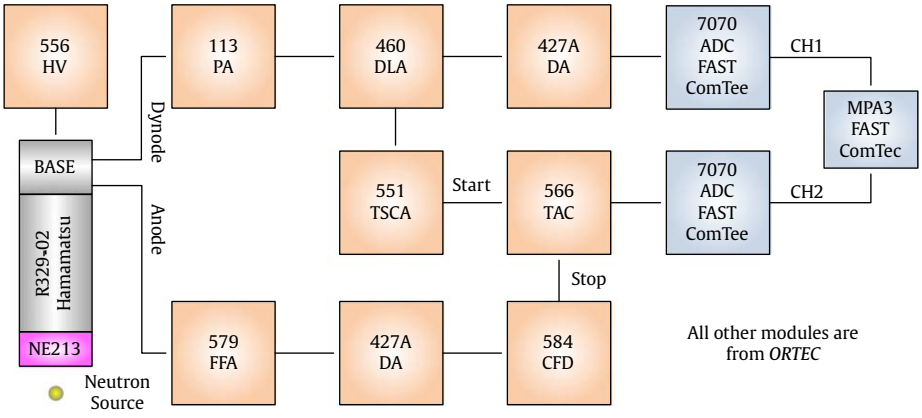

Fig. 4. A zero-crossing pulse shape discrimination circuit.

et al., 2006):

$$MSE = \sqrt{\frac{1}{m}\sum_{j=1}^{m}(\Phi_E(E)_j^{ANN} - \Phi_E(E)_j^{ORIGINAL})^2} \quad (6)$$

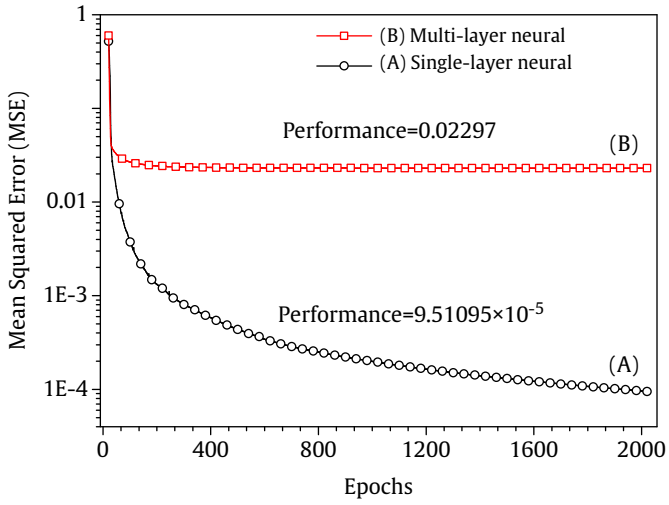

Fig. 5. Convergence graph for linear and non-linear neural nets.

where the index $j = 1, 2,\ldots,m$ is the number of neutron energy intervals (or output neurons).

The Epoch presents the set of training (input and/or target) vectors to a network and the calculation of new weights and biases (Demuth and Beale, 2002).

2.2. Experimental setup

The detector assembly consists of a 6 cm length and 6 cm diameter commercial NE213 liquid scintillator cell, coupled to a R329-02 photomultiplier tube (PMT) and voltage divider (manufactured by HAMAMATSU) was used for the experiment. A conventional measuring system of zero-crossing pulse shape discrimination and multi-parameter data acquisition (Fig. 4) was used to process the signals from a photomultiplier tube and to separate photon signals from neutron induced ones.

Two neutron sources, 3.7 GBq (100 mCi) ^{241}Am–Be and 37 KBq (10 μCi) ^{252}Cf neutron source, were positioned at a distance of 32 cm from the center of detector on its central axis. To decrease the effect of backscattering neutrons, the source and detector were positioned 3–4 m from the walls and 2.5 m high above the ground. The room temperature was 20–25 °C during measurements.

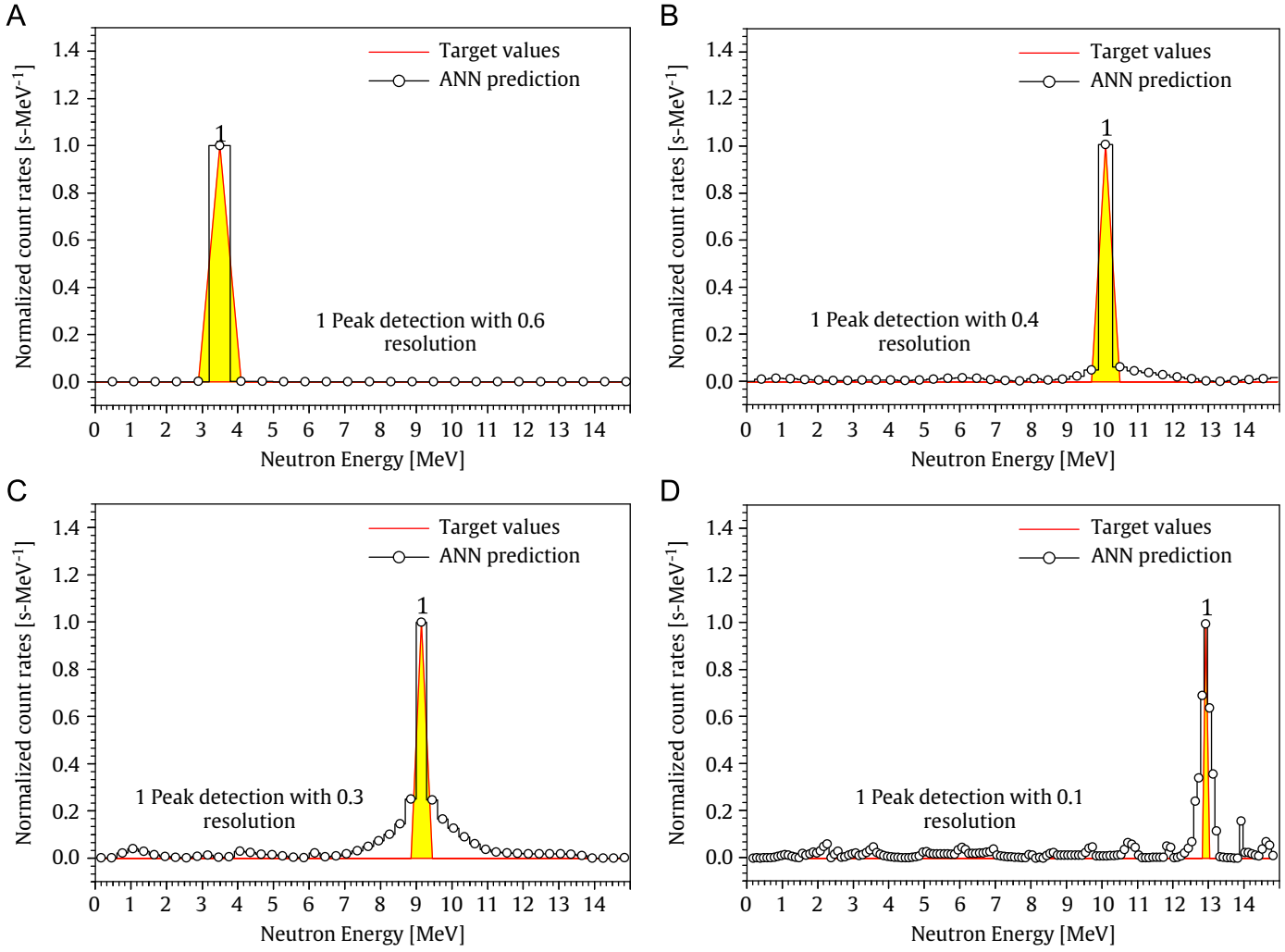

Fig. 6. The response of the implemented linear neural net for mono-energetic sources with various resolutions (A) 0.6 MeV, (B) 0.4 MeV, (C) 0.3 MeV and (D) 0.1 MeV).

3. Results and discussion

3.1. Unfolding monoenergetic spectra

The ANN was tested unfolding monoenergetic neutron spectra. The neural network can be implemented in nonlinear (multi-layer) or linear (single-layer) models. Here, the multi-layer is implemented and the sigmoid tangent (TanSig) is used for the neurons in a hidden layer and the output layers transfer function. Moreover, the resilient back-propagation algorithm is implemented for the weight adaptation. The number of output neurons in the output layer are varied depending on the accuracy of the input vectors generated by the Monte Carlo code, SCINFUL.

The ANN with a topology I:10:O (in our simulation, I and O correspond with the response matrix dimensions that is generated by SCINFUL, 343 and 29, respectively) shows the best performance ($MSE = 0.02297$), as it is noticed in Fig. 5(B) where convergence is reached approximately after 2000 epochs.

On the other hand, as it can be seen from Fig. 5(A), the single layer neural net with the same topology as the mentioned multi-layer (in our simulation 343:29, no hidden neurons) has a more efficient performance ($MSE = 9.51095 \times 10^{-5}$) improvement than the multi-layer neural net. Hence, in this study, our investigations have been focused on the single layer neural nets.

In the case of the linear neural net, the single layer perceptron with the resilient back-propagation algorithm is used. The number of input neurons considered for the output layer of the network is varied depending on the output resolution for the training vectors generated by the Monte Carlo SCINFUL code.

The results of the linear networks for mono-energetic spectra are shown in Fig. 6. In this case, the SCINFUL code has been used to generate the vectors in four distinct resolutions including 0.6 (Fig. 6(A)), 0.4 (Fig. 6(B)), 0.3 (Fig. 6(C)) and 0.1 (Fig. 6(D)) in the training phase. The *MSE* between the target values and ANN prediction in Fig. 6 was 1.00×10^{-10}, 0.001, 0.0024 and 0.0044, respectively.

In all implementations, the neural nets are trained, using only the mono-energetic spectra of several resolutions in specific steps.

Fig. 7 shows the results of the multi-peak spectra. In this simulation, the single-layer neural net had 128 neurons in the input layer (determined by the sampling rate of our data) and 25 neurons in the output layer (determined by the considered resolutions of the generated data by SCINFUL). All peaks have the same amplitude in the input.

3.2. Comparison with FORIST code

Finally, the results of the ANN were benchmarked based on the results of the FORIST code. Fig. 8 shows the results of the proposed method in comparison with the FORIST code for a ^{241}Am–Be neutron source. Fig. 9 illustrate the results of the unfolded neutron spectra for a ^{252}Cf neutron source, whilst the fitted curve indicates the spontaneous fission spectra. Eq. (7) indicates the

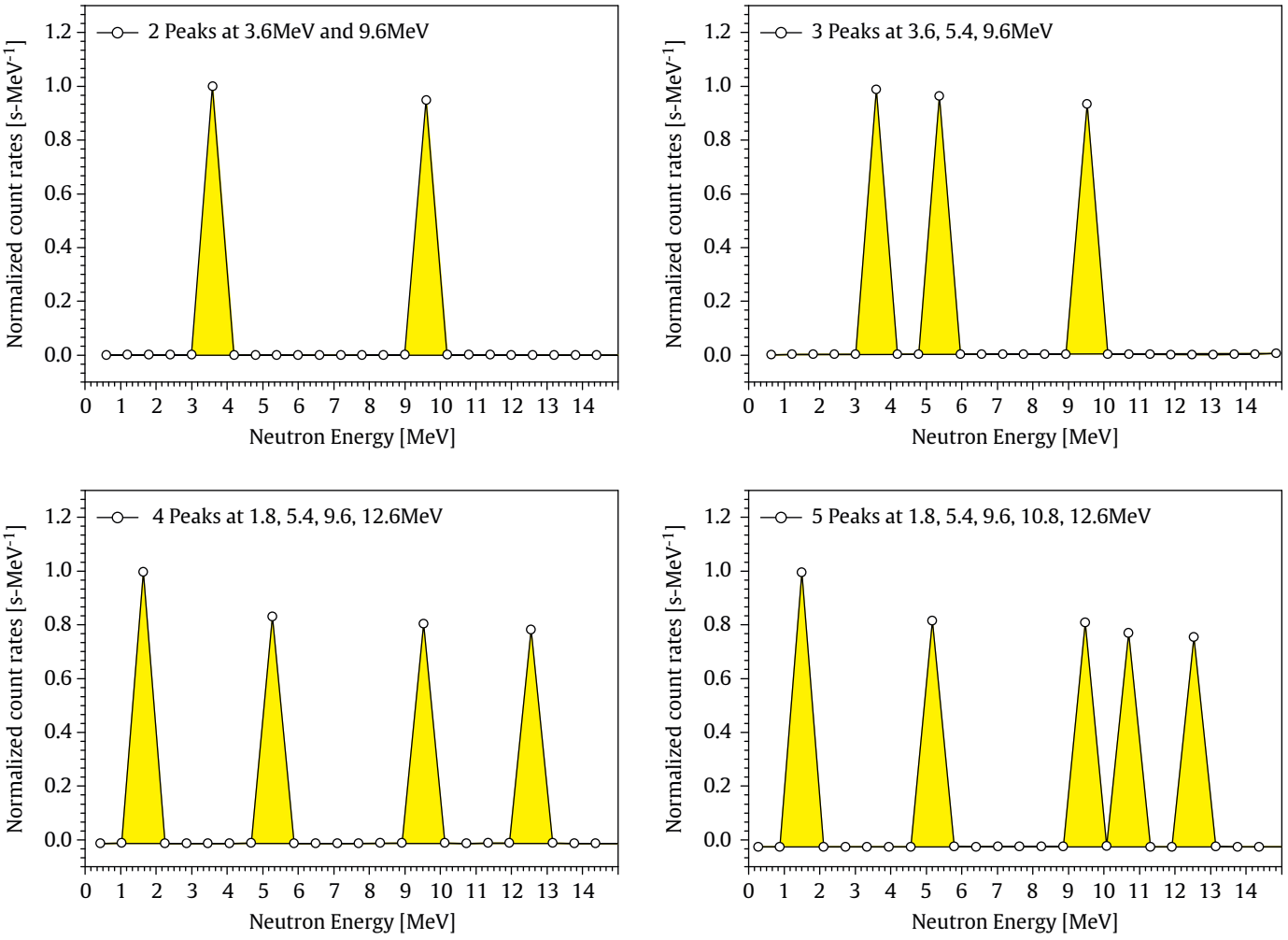

Fig. 7. The single layer neural net for predicting the vectors of multi-energetic constructed inputs.

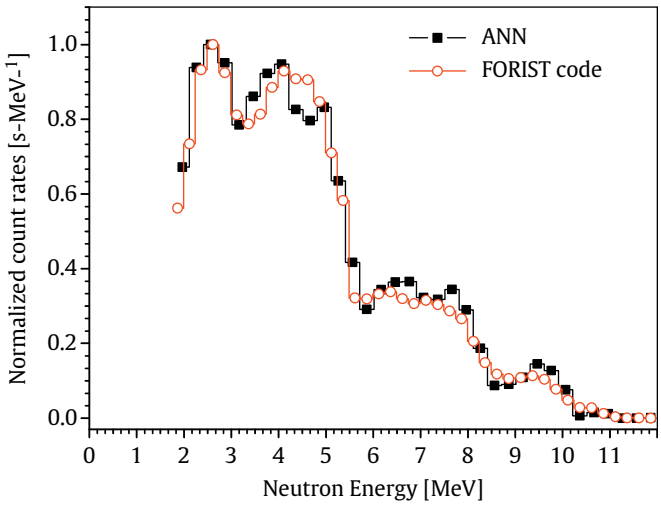

Fig. 8. Unfolded neutron spectra for ^{241}Am–Be neutron source ANN vs. FORIST results.

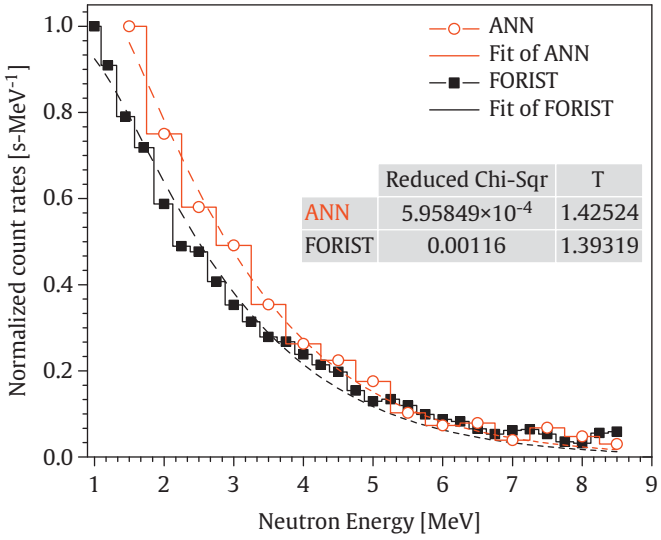

Fig. 9. Unfolded neutron spectra for ^{252}Cf neutron source.

Maxwellian fission spectrum, where T is a constant and C is a normalization factor. By fitting a curve to the calculated data, the values of $T = 1.42524$ and 1.39319 are obtained for ANN and FORIST respectively, which is in good agreement with reference value $T = 1.42$ (Hambsch et al., 2005). Curve-fitting was performed using Origin 8.0 software (Origin Lab Corp., North Hampton, MA, USA). Since the number of energy bins of FORIST unfolded spectrum was different from the number of energy bins used to unfold the spectrum using ANN, a chi–square test between the unfolded spectra with Maxwell fission spectrum was been used.

$$\frac{dN}{dE} = CE^{0.5}\exp(-E/T) \tag{7}$$

4. Conclusions

In this paper, two models of artificial neural network (multi-layer and single layer) have been developed for unfolding the neutron spectra. The ANN's are trained using the neutron mono-energetic spectra and are tested in both single peak and multi-peak energies in their targets. Three transfer functions were investigated for the neural networks. The simulation results show that the single layer neural network is strongly compatible with the unfolding problem in comparison with the multi-layer neural network. We showed that the Satlins transfer function of the linear (single-layer) form and with the omitted bias term have a better result in comparison with Tansig (sigmoid tangent) and Purelin methods. The omission of bias term leads to better convergence of ANN. The capability of ANN was tested using experimental data obtained by measuring neutron spectra of ^{241}Am–Be and ^{252}Cf sources. Both unfolded spectra are in agreement with the result provided in the literature for neutron spectroscopy. For ^{252}Cf data, a Maxwellian spectrum was fitted to results and an excellent agreement was observed. Furthermore for both neutron sources unfolding has been done using FORIST code. The results of ANN are also in agreement with FORIST simulation.

The simple structure of the proposed ANN (a linear ANN with a simple transfer function) is exceedingly susceptible to be programmed in a programmable chip such as FPGA. Although it has this benefit, the sensitivity of the ANN on the precision of learning data (response matrix) is a critical point that has to be considered. In fact, the ANN maps its inputs to its outputs according to the weights which are modified using the learning data (here response matrix). Hence, the precision of the learning data can strongly affect mapping.

Acknowledgments

The authors would also like to extend their thanks to unknown reviewers of the manuscript for their valuable contributions.

References

Avdic, S., Pozzi, S.A., Protopopescu, V., 2006. Detector response unfolding using artificial neural networks. Nucl. Instrum. Method Phys. Res. A 565, 742–752.
Burrus, W.R., 1976. FERD and FERDOR type unfolding codes. Report ORNL/RSIC–40, 2–23.
Cecil, R.A., Anderson, B.D., Madey, R., 1979. Improved predictions of neutron detection efficiency for hydrocarbon scintillators from 1 MeV to about 300 MeV. Nucl. Instrum. Methods 161, 439–447.
Demuth, H., Beale, M., 2002. Neural network toolbox for use with Matlab. User Guide Version 4. The Mathworks, Inc.
Dickens, J.K., 1988. SCINFUL: a Monte Carlo based computer program to determine a scintillator full energy response to neutron detection for En between 0.1 and 80 MeV. Part 1: User's manual and FORTRAN program listing. Report ORNL–6462, Oak Ridge. Part 2: Program development and comparisons of program predictions with experimental data. Report ORNL–6463, Oak Ridge.
Hagan, N.J., Demuth, M.T., Beale, M.H., 1996. Neural Network Design. PWS Publishing, Boston, MA.
Hambsch, F.-J., Tudorab, A., Vladucab, G., Oberstedta, S., 2005. Prompt fission neutron spectrum evaluation for ^{252}Cf (SF) in the frame of the multi-modal fission model. Annals of Nuclear Energy 32, 1032–1046.
Johnson, R.H., 1975. A user's manual for COOLC and FORIST. PNE–75–107.
Johnson, R.H., Ingersoll, D.T., Wehring, B.W., Dorning, J.J., 1977. NE–213 neutron spectrometry system for measurements from 1.0 to 20 MeV. Nucl. Instrum. Method A 145, 337–346.
Klein, H., Neumann, S., 2002. Neutron and photon spectrometry with liquid scintillation detectors in mixed fields. Nucl. Instrum. Method A 476, 132–142.
Knoll, G.F., 2000. Radiation Detection and Measurement, third edition. Wiley, New York.
Koohi-Fayegh, R., Green, S.J., Crout, N.M., Taylor, G.C., Scott, M.C., 1993. Nucl. Instrum. Method A, 329–369.
Meigo, S., 1997. Measurements of the response function and the detection efficiency of an NE213 scintillator for neutrons between 20 and 65 MeV. Nucl. Instrum. Method A 401, 365–378.
Mullens, J.A., Edwards, J.D., Pozzi, S.A., 2004. Analysis of scintillator pulse height for nuclear material identification. In: Institute of Nuclear Materials Management 45th Annual Meeting, July 18–22, Orlando, FL.
Rasolonjatovo, H.D., Shiomi, T., Kim, E., Nakamura, T., Nunomiya, T., Endo, A., Yamaguchi, Y., Yoshizawa, M., 2002. Development of a new neutron monitor using a boron-loaded organic liquid scintillation detector. Nucl. Instrum. Method A 492, 423–433.
Rosenblatt, F., 1961. Principles of Neurodynamics. Spartan Press, Washington D.C.
Sanna, R., O'Brien, K., 1971. Monte-Carlo unfolding of neutron spectra. Nucl. Instrum. Method A 91, 573–576.

Sanna, R.S., 1981. A manual for BON: A code for unfolding multisphere spectrometer neutron measurements. In: EML–394.

Satoh, D., Sato, T., Endo, A., Yamaguchi, Y., Takada, M., Ishibashi, K., 2005. Study on response function of organic liquid scintillator for high-energy neutrons. In: International Conference on Nuclear Data for Science and Technology, AIP Conference Proceedings, vol. 769, pp. 1680–1683.

Stallmann, F.W., 1985. LSL–M2: a computer program for least-squares logarithmic adjustment of neutron spectra. In: NUREG/CR–4349, ORNL/TM–9933.

Vega-Carrillo, H.R., Hernández-Dávila, V.M., Manzanares-Acuña, E., Mercado, G.A., Iñiguez, M.P., Barquero, R., Palacios, F., Méndez, R., Arteaga, T., Ortiz, J., 2006. Neutron spectrometry using artificial neural networks. Radiat. Meas. 41, 425–431.

Vega-Carrillo, H.R., Hernández-Dávila, V.M., Manzanares-Acuña, E., Gallego, E., Lorente, A., Iñiguez, M.P., 2007. Artificial neural networks technology for neutron spectrometry and dosimetry. Radiat. Prot. Dosimetry 126 (1–4), 408–412.